Microchimica Acta (2020) 187: 85
https://doi.org/10.1007/s00604-019-4030-4

ORIGINAL PAPER

Fluorometric determination of lead(II) by using aptamer-functionalized upconversion nanoparticles and magnetite-modified gold nanoparticles

Min Chen[1] · Mehedi Hassan[1] · Huanhuan Li[1] · Quansheng Chen[1]

Received: 9 June 2019 / Accepted: 11 November 2019 / Published online: 2 January 2020

Abstract

A fluorescent nanoprobe for Pb(II) has been developed by employing aptamer-functionalized upconversion nanoparticles (UCNPs) and magnetic Fe_3O_4-modified (MNPs) gold nanoparticles (GNPs). First, aptamer-functionalized UCNPs and aptamer-functionalized magnetic GNPs were synthesized to obtained the fluorescent nanoprobe. The particles were combined by adding a complementary ssDNA. In the absence of Pb(II), the UCNPs, MNPs and GNPs are linked via complementary base pairing. This led to a decrease in the green upconversion fluorescence peaking at 547 nm (under 980 nm excitation). In the presence of Pb(II), the dsDNA between UCNPs and MNPs-GNPs is cleaved, and fluorescence recovers. This effect allows Pb(II) to be quantified, with a wide working range of 25–1400 nM and a lower detection limit of 5.7 nM. The nanoprobe gave satisfactory results when analyzing Pb(II) in tea and waste water.

Keywords UCNPs · MNPs-GNPs · DNAzyme · Nanoprobe · FRET · Pb^{2+}

Introduction

Lead is widely used in batteries, fertilizers and plastic stabilizers, resulting in water, soil and air pollution [1, 2]. Pb^{2+} not only acts as an environmental pollutant but also adversely affects human health. The maximum residual limits of Pb^{2+} set by the World Health Organization (WHO) and the U.S. Environmental Protection Agency (EPA) for drinking water are about 35.7 nM [3] and 53.6 nM [4], respectively. Various analytical techniques such as colorimetric [5, 6], fluorescence [7, 8] and surface-enhanced Raman scattering (SERS) [9] have been developed to detect Pb^{2+} with low concentration. However, the fluorescence method has become an influential method for its high selectivity and sensitivity. Nowadays, many fluorescence chemosensors have been successfully developed for the detection of Pb^{2+}. However, the most fluorescence chemosensors consist of organic fluorescent dyes, which have some disadvantages like toxicity, prolonged synthesis time, interference of background and poor water solubility, which limit the prospect of application in the detection of real sample. For instance, Y Xiang et al. developed a 2-amino-5,6,7-trimethyl-1,8-naphthyridine fluorescence sensor (excitation/emission = 358/405 nm) for detection of Pb^{2+} with LOD of 4 nM [10], however, the dye used is poisonous and the fluorescence spectra cannot abstain from background interference; S Zhan et al. reported a label free fluorescence sensor (excitation/emission = 490/535 nm) for Pb^{2+} with LOD of 13.5 nM [11], which is also bear the weakness of background. Therefore, a new fluorescence sensor with low background interference and high sensitivity is greatly needed to develop for Pb^{2+} detection.

Compared to the fluorescent dyes, rare-earth-doped upconversion nanoparticles (UCNPs) with high anti-Stokes shift, low auto-fluorescence background and high penetration depth can convert near infrared long-wavelength excitation radiation to shorter visible wavelength [12–14]. In addition, upconversion nanoparticles are less toxic and can be modified into water soluble [15, 16]. Due to the above features, UCNPs has been successfully applied for the detection of metal ions

Electronic supplementary material The online version of this article (https://doi.org/10.1007/s00604-019-4030-4) contains supplementary material, which is available to authorized users.

✉ Huanhuan Li
876865759@qq.com

✉ Quansheng Chen
qschen@ujs.edu.cn

[1] School of Food and Biological Engineering Jiangsu University, Xuefu Road 301, Zhenjiang 212013, People's Republic of China

[17, 18] based on the fluorescence quenching or fluorescence recovering by fluorescent acceptor. Therefore, it is very important to select a suitable fluorescent acceptor to develop an optimum probe for Pb^{2+} detection.

Gold nanoparticles (GNPs) exhibit their unique optical properties [19, 20] such as high extinction coefficients, colors arising from GNPs and strongly distance-dependent optical properties. In addition, the GNPs possess superior chemical properties such as size, mild surface chemistry and exhibit low toxicity [21]. Owing to the above advantage, GNPs have been applied in colorimetric assays for the detection of metal ions. MNPs [22, 23] have gained increasing interest, due to its low cost, wide availability, high stability, easily chemically modifiable surfaces and convenient magnetic separation properties [24]. Consequently, the composite assembly of MNPs and GNPs as fluorescent acceptor is suitable.

DNAzyme (catalytic strand) mainly consists of nucleic acid, which can either bind with target molecules or implements catalytic reactions with the ability to recognize metal ions [2]. Besides, DNAzyme has successfully been applied in the detection of many metal ions, like, Zhang et al. developed a biosensor based on DNAzyme decorated Au@Ag core-shell nanoparticles for mercury [25]. Some related research works [10, 11, 26] using DNAzyme to develop a biosensor for the detection of Pb^{2+} have also been reported. These fluorescence biosensors cannot detect Pb^{2+} in complex samples due to their unstable optical properties and their detection limit also need to improve. Therefore, developing a new nanoprobe based on DNAzyme is significant.

In this paper, we have devised and prepared an "off-on" upconversion fluorescent nanoprobe that consists of aptamer-functionalized UCNPs and MNPs-GNPs for Pb^{2+} detection. Without the addition of Pb^{2+}, the link between UCNPs and MNPs-GNPs formed by the complementary pairing of aptamer, led to the distance between UCNPs and MNPs-GNPs less than 10 nm, causing the occurrence of FRET. Upon addition of Pb^{2+}, Pb^{2+} captured by DNAzyme and resulted in the catalytic hydrolysis of the oligonucleotide, which diminished the effect of FRET, consequently recovering the fluorescence. This novel fluorescent nanoprobe not only has a wide linear range but also exhibits a low detection limit for the determination of Pb^{2+}.

Experimental

Materials

$YCl_3 \cdot 6H_2O$(99.99%), $YbCl_3 \cdot 6H_2O$(99.99%), $GdCl_3 \cdot 6H_2O$(99.99%), $HoCl_3 \cdot 6H_2O$ (99.99%), 1-octadecene (> 90%) and oleic acid (> 90%), and chloroauric acid trihydrate ($HAuCl_4 \cdot 3H_2O$, 99.9%) were purchased from Sigma-Aldrich (Shanghai, China www.sigmaaldrich.com). Phosphate-buffered saline with 0.9% NaCl (PBS) (10 mM, pH = 7.4), 3-aminopropyltrimethoxysilane, tetraethyl orthosilicate (TEOS, > 98%), sodium hydroxide (NaOH, 96%), ammonium fluoride (NH_4F, 98%), iron chloride hexahydrate, avidin and other reagent were obtained from Alfa Aesar (www.alfa.com). The catalytic strand 5′-Biotin-CGA TCA CTA ACT ATr AGG AAG AGA TG-HS-3′ (Apt1) and complementary strand 5′-NH_2-TGA GTG ATA AAG CTG GCC GAG CCT CTT CTC TAC-3′ (Apt2) were purchased from Sangon Biotechnology Co., Ltd. (Shanghai, China).

Characterization

he shape and size of the silica-coated UCNPs, MNPs and GNPs were characterized by a Tecnai G2 F30 transmission electron microscopy (TEM) at an accelerated voltage of 120 kV. A Siemens D5005 instrument (Bruker AXS, Ltd., Germany) was used to record the X-ray diffraction (XRD) pattern. The infrared (IR) spectra were recorded by a Nicolet Nexus 470 Fourier transform infrared spectrophotometer (Thermo Electron Co., U.S.A.). The absorption spectra were acquired by a Shimadzu UV-1800 UV-Vis spectrophotometer (Shimadzu, Japan). The zeta potentials were measured using Malvern Zetasizer Nano (Malvern Instruments Ltd., U.K).

Synthesis of upconversion nanoparticles (UCNPs)

Oleic acid-capped $NaYF_4$: Gd, Yb, Ho nanoparticles (OA-UCNPs) were prepared according to the previous literature [27, 28] with some modification and detail procedure has been assimilated in the supporting information. Water-soluble upconversion nanoparticles were prepared with the modification of amino group using the following procedures: 100 mg of UCNPs and 40 mL of ethanol mixed by ultrasound for 20 min in 100 mL conical flask. Then the mixture was heated to 35 °C under continuous stirring for 10 min. Thereafter, 10 mL of pure water and 1.2 mL of ammonia solution were added respectively to the above mixture and heated to 60–70 °C. After that, 100 μL of tetraethyl orthosilicate added slowly under continuous stirring and kept for 8–10 h in the same condition. Subsequently, 100 μL of 3-aminopropyltriethoxysilane was added with the above mixture and kept for another 3 h under the same condition to yield amino-functionalized UCNPs. Finally, the amino-functionalized UCNPs solution was washed by water-ethanol (1:3) three times and dried in a vacuum oven at 60 °C for 6 h. .

Synthesis of surface modification Fe_3O_4 magnetic nanoparticles (MNPs)

Amine-functionalized Fe_3O_4 MNPs was fabricated according to the previous work [14]. First, 3.2 g of 1, 6-hexanediamine,

1.0 g of anhydrous sodium acetate and 1.0 g of $FeCl_3$ $6H_2O$ were dissolved in 15 mL of glycol. Then, the mixture was heated to 50 °C to obtain a homogeneous colloidal solution, followed to transfer into a Teflon-lined autoclave and kept at 198 °C for 6 h to form amine-functionalized Fe_3O_4 MNPs. Finally, the products were washed with ethanol-water three times and dried in a vacuum oven.

Synthesis of gold nanoparticles (GNPs)

GNPs was obtained according to the previous literature [29] with appropriate modifications and detail procedure has been assimilated in the supporting information.

Preparation of aptamer-functionalized upconversion nanoparticles (UCNPs)

The aptamer-functionalized UCNPs was fabricated applying the classical glutaraldehyde method. First, 1.25 mL of glutaraldehyde and 10 mg of amino-modification UCNPs were dispersed in 5 mL of PBS by ultrasound for 30 min. After reaction for 1 h, the UCNPs was washed by PBS three times and re-dispersed in 5 mL of PBS. Then, 0.5 mL of 200 mM Apt2 was added to the UCNPs solution and reacted at room temperature for 6 h. Finally, the UCNPs solutions were washed and re-dispersed in 5 mL of PBS.

Preparation of aptamer-functionalized GNP-MNPs

The procedure for the avidin-modified MNPs was adapted from reported literature [14, 30]. Briefly, 10 mg of MNPs dispersed in 5 mL of PBS then added 1.25 mL of 25% glutaraldehyde to the above mixture and kept for 2 h at room temperature. Then, MNPs were magnetically separated and subsequently washed with PBS. Thereafter, 2 mL of 5 mg/mL avidin solution was added to the above solution and kept for 12 h at room temperature. Finally, the yielded avidin-modified UCNPs was washed with PBS three times and dried in a vacuum oven at 37 °C for 12 h.

The aptamer-functionalized GNP-MNPs was synthesized according to our previous literature [31]. First, 0.5 mL of 200 mM Apt1 was added to 10 mg of avidin-modified MNPs solution and incubated for 6 h at room temperature to fabricate MNPs-Apt1. Then the MNPs-Apt1 was magnetically separated and re-dispersed in 4.0 mL of PBS. After that, 1.0 mL of GNPs was poured into the mixture and incubated at 50 °C for 16 h. Thereafter, 0.1 M of NaCl and 10 mM of PBS buffer were added to the above mixture and reacted for another 40 h. Finally, the GNPs-MNPs was magnetically separated and stored at 4 °C. The concentration of GNPs-MNPs was calculated according to the concentration of MNPs.

Fabrication of the nanoprobe

The UCNPs-GNPs-MNPs nanoprobe was synthesized as follows. 200 μL of 1.0 mg/mL aptamer-functionalized GNPs-MNPs was mixed with 200 μL of 1.0 mg/mL aptamers-modified UCNPs and reacted for 10 min at 37 °C to fabricate UCNPs-GNPs-MNPs nanoprobe. Then, the nanoprobe was magnetically separated and washed with PBS. Finally, the nanoprobe was re-dispersed in PBS buffer solution.

Lead(II) detection

$Pb(NO_3)_2$ stock solution was used for Pb^{2+} sensitivity studies. Various concentrations of Pb^{2+} solution were prepared from the stock solution using serial dilution to determine the sensitivity limits of the UCNPs-GNPs-MNPs. The fluorescence detection of aqueous Pb^{2+} was performed at optimal conditions. Briefly, 200 μL of Pb^{2+} with different concentrations (25, 50, 100, 200, 400, 600, 800, 1000 nmol/L) were added separately to 3 mL glass bottle containing 200 μL of UCNPs-GNPs-MNPs solution. The glass bottle was subsequently shaken for 10 min to confirm the reaction. For the selectivity and practical assay, all samples were analyzed in the same condition. The selectivity over other metal ions (Cd^{2+}, Cr^{3+}, Ba^{2+}, Zn^{2+}, Ca^{2+}, Mn^{2+}, Mg^{2+}, Fe^{2+}, Co^{2+}, Ni^{2+}, Cu^{2+}, Hg^{2+}) under same conditions were investigated. To confirm the selectivity of our developed method, 200 μL of various metals ion were prepared and added to 200 μL of UCNPs-GNPs-MNPs solution. Selectivity was tested as follows: 200 μL of mixed metal ions (1 μM Pb^{2+} and 100 μM one of the other metal ions) was prepared and added to 200 μL of UCNPs-GNPs-MNPs solution.

Detection of lead(II) in spiked real samples

Waste water samples obtained from domestic and industrial waste water sources and centrifuged at 10000 rpm for 30 min. Spiked samples were prepared by adding Pb^{2+} at specific concentrations. Then spiked samples were detected using the UCNPs-MNPs-GNPs nanoprobe. Black tea was purchased from local supermarket and pretreatment of tea was followed by a previous method [32] with a little modification. First, the tea sample was dried in an oven at 35 °C, then 1.0 g of tea sample was digested with a mixture of concentrated HNO_3 (4 mL) and $HClO_4$ (1 mL) for 1 h and filtered under atmospheric pressure. Afterwards, various concentrations of Pb^{2+} were mixed with the filtrate. Finally, the filtrate was detected using our developed method.

Results

Characterization

To comfirm the shape, size, crystal form, zeta potential and surface modification of UCNPs, MNPs and GNPs, we conducted a series of characterization and the results are shown in Fig. 1. As seen from the TEM image, as synthesized UCNPs was covered by uniform silicon shell with good dispersibility and the average size of the particle was 35 nm (Fig. 1a). The TEM image also revealed that GNPs and MNPs were spherical in shape with an average diameter of 20 nm and 200 nm respectively and well dispersed as captured in Fig. 1b, c. Additionally, the relative zeta (ζ)-potential of UCNPs, GNPs and MNPs were measured and the results are shown in Fig. 1d. Amino-modified UCNPs was positively charged with zeta potential of +12.32 mV. After aptamer-modification, the zeta potential changed to +23.67 mV. The opposite zeta potential was found between GNPs (−11.79 mV) and MNPs (+36.72 mV), but after the conjugation by the aptamers, the zeta potential of MNPs-GNPs was positively charged with +18.87 mV, indicated that the UCNPs-MNPs-GNPs nanoprobe formed by the bases complement not by the electrostatic adsorption.

The crystal structure and phase purity of UCNPs and MNPs were determined by XRD. The diffraction peaks of the UCNPs (Fig. 2a) were well agreed with the calculated values of standard hexagonal $NaYF_4$ phase (JCPDS no.49–1896), indicate that synthesized UCNPs had crystalline hexagonal phase. The relative intensities of all diffraction peaks of MNPs corresponded to the phase structure of magnetite (JCPDS no. 88–0866) as shown in Fig. 2b.The surface properties of UNCPs and MNPs were determined by FT-IR spectroscopy. As presented in Fig. 2c, the characteristic peaks at 3412 cm^{-1} was assigned to the stretching vibration of hydroxide radicals (-OH) of oleic acid on the surface of UCNPs; 2923 cm^{-1}, 2847 cm^{-1} and 1579 cm^{-1} and 1431 cm^{-1} corresponded to the stretching vibration absorption peaks of hydroxide radicals (-CH_2-) and the carboxylic group (-COOH) of oleic acid, respectively (curve a in Fig.2c (b)) [33]. After surface modification, the stretching vibration of the Si-O (1614 cm^{-1}) band and stretching and bending vibration of amine groups (1102 cm^{-1}) appeared, indicated that the UCNPs was successfully modified with NH_2 (curve a in Fig. 2c (c)) [34]. The peak appeared at 1391 cm^{-1} and 1047 cm^{-1} were ascribed to the rocking vibration of N-H in the amine and stretching vibration of –CH–; while the characteristic peak at 1627 cm^{-1} was attributed to the scissor bending vibration of amine group. The peak appeared at 580 cm^{-1} was attributed to the Fe-O vibrations (curve a in Fig. 2c (a)) [14]. The data of UV-Vis spectrophotometer approved that MNPs-GNPs and UCNPs were successfully modified by aptamer (Fig. 2d).

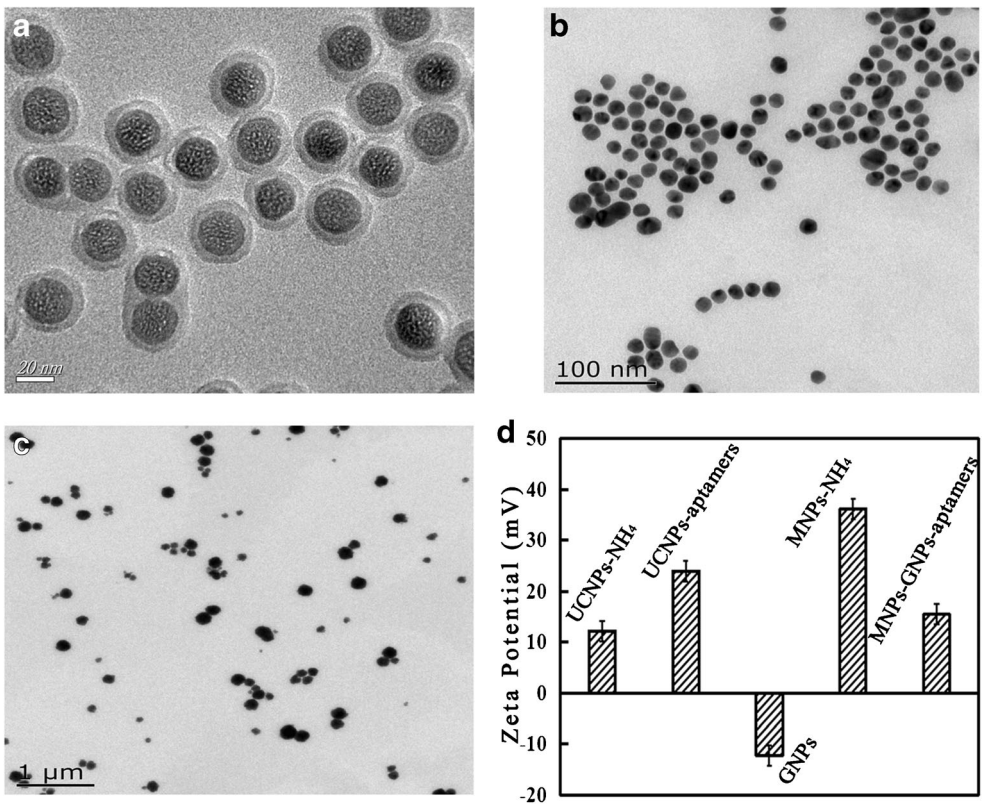

Fig. 1 TEM image of amino-modified upconversion nanoparticles (UCNPs) (**a**), gold nanoparticles (GNPs) (**b**) and Fe_3O_4 magnetic nanoparticles (MNPs) (**c**). ζ-Potential of UCNPs-NH_4, UCNPs-aptamer, (GNPs), MNPs-NH_4, MNPs-GNPs-aptamer (**d**)

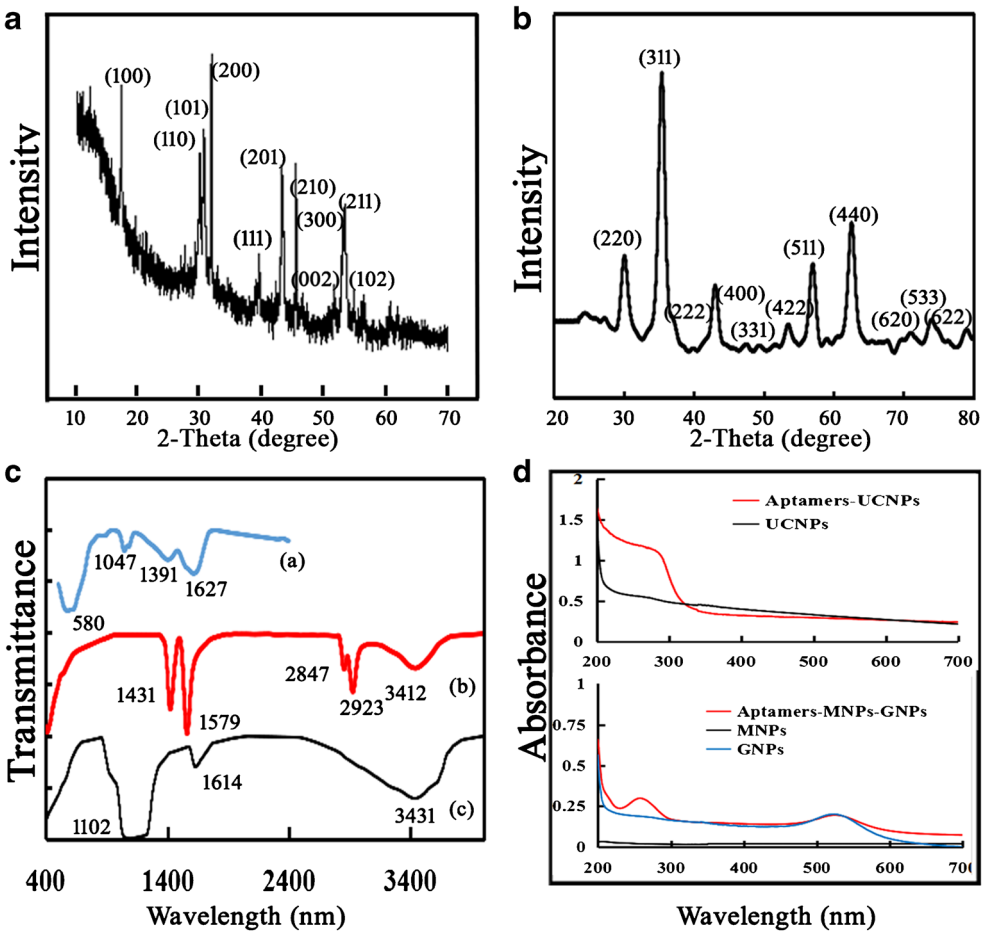

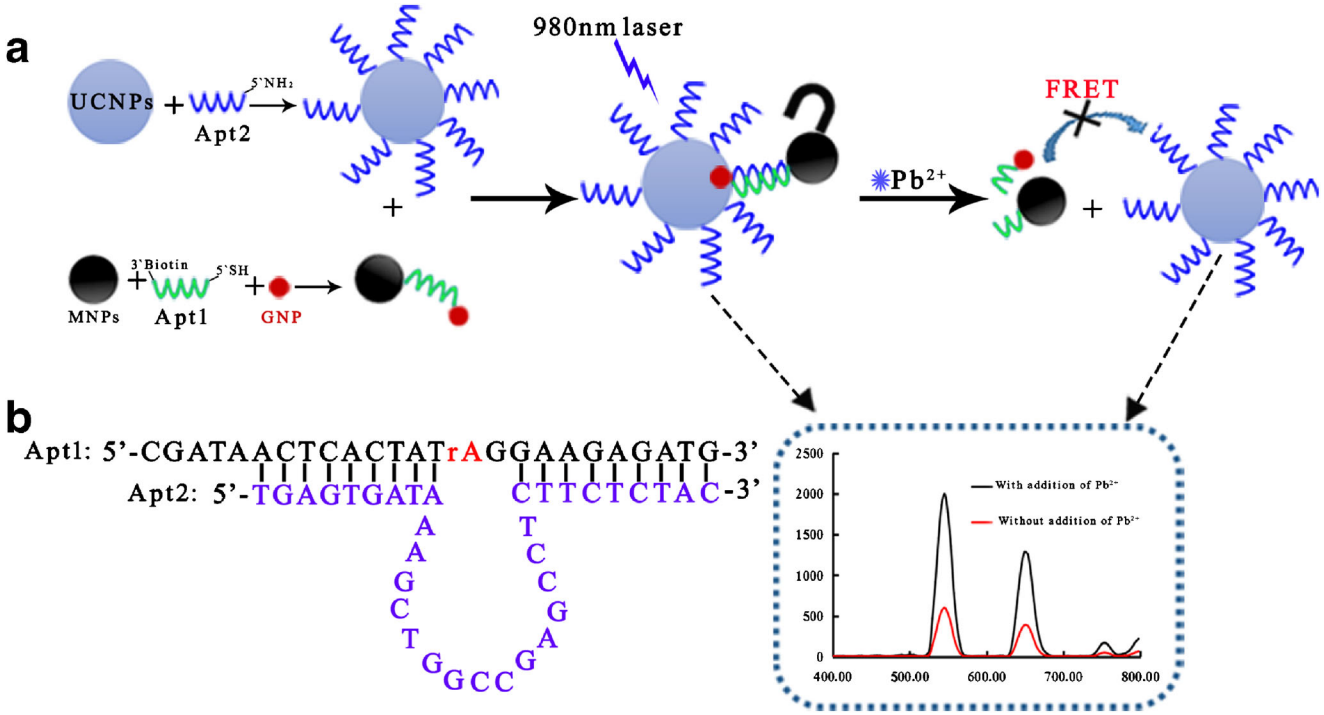

Fig. 2 XRD patterns of UCNPs (**a**) and MNPs (**b**). **c** FT-IR spectra of MNPs, UCNPs and amino-modified UCNPs. **d** UV-Vis spectra of the UCNPs, GNPs and MNPs before and after aptamer modification

Fig.3 **a** Schematic presentation of fluorescent nanoprobe based on fluorescence resonance energy transfer (FRET) between UCNPs and GNPs-MNPs for detection of Pb^{2+}. **b** The structure formula of combined UCNPs and MNPs-GNPs

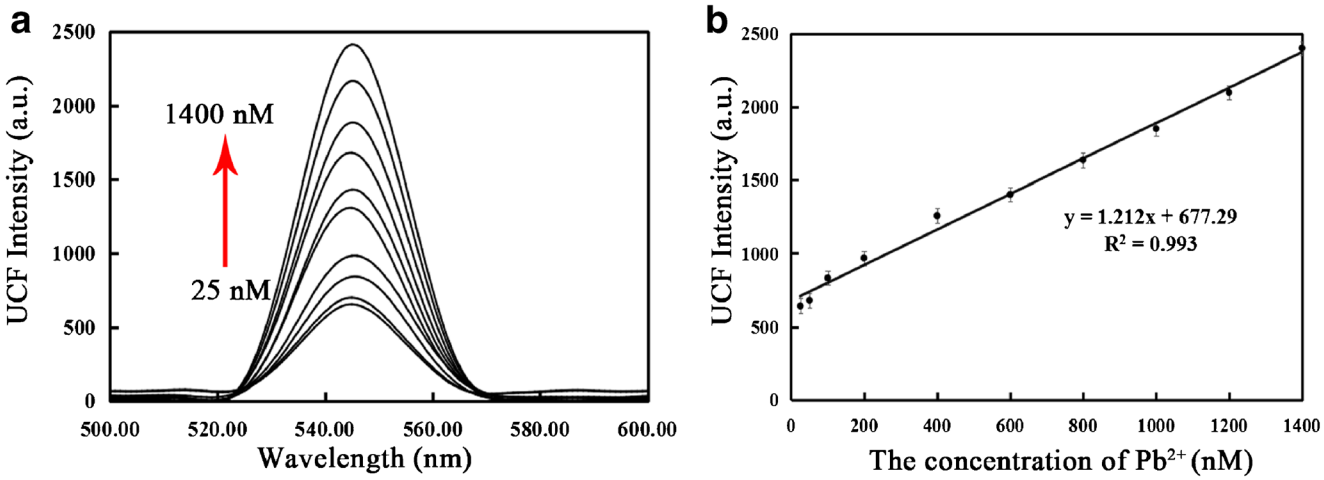

Fig. 4 **a** Upconversion fluorescence spectra of UCNPs-MNPs-GNPs under 980 excitation with addition of different concentration of Pb^{2+}. **b** The plot of upconversion fluorescence spectra intensity at 547 nm versus Pb^{2+}

After aptamer modification, the new absorption peak at 280 nm appeared, confirmed that UCNPs and GNPs-MNPs were modified by aptamer successfully.

Principle of the "turn-on" upconversion fluorescent nanoprobe for lead(II)

The detection mechanism of the "turn-on" for Pb^{2+} based on upconversion fluorescent nanoprobe is described in detail in Fig.3. A single-stranded aptamer (Apt2) was modified with UCNPs. Hitherwards, the MNPs and GNPs were modified and linked by the Apt1. In the absence of Pb^{2+}, UCNPs was combined with MNPs-GNPs by the interaction of aptamer and the fluorescence resonance energy kept transferring to the MNPs-GNPs.

This is attributed to the overlap between the fluorescence spectrum of UCNPs and the absorption spectrum of MNPs-GNPs in 500–600 nm that cause FRET between them. In the presence of Pb^{2+}, the catalytic strand was cut off by Pb^{2+}. Meanwhile, the base pairs break, led to the separation of UCNPs and MNPs-GNPs, resulted in the quenched fluorescence restoration through removing the effect of FRET. Therefore, the Pb^{2+} concentrations were monitored by the fluorescence at 547 nm.

Optimization of experimental conditions

In order to obtain better sensing performance for Pb^{2+} detection, the following parameters were optimized: (a) Optimal concentration ratio of UCNPs and MNPs-GNPs: 1.0 mg/mL UCNPs and 1.0 mg/mL MNPs-GNPs; (b) Best hybridization time between aptamer-functionalized UCNPs and aptamer-functionalized MNPs-GNPs:10 min; (c) Best reaction time after addition of Pb^{2+}: 4 min. All the experiments were conducted at room temperature.

Determination of lead(II)

The fluorescence intensity of the assay solution was investigated using 200 μL UCNPs-MNPs-GNPs conjugates upon addition of different concentrations of Pb^{2+} (25, 50, 100, 200, 400, 600, 800, 1000 nmol/L) under the optimized conditions, as shown in Fig.4. Figure 4a shows upconversion fluorescence spectra against the concentration of Pb^{2+} in the homogeneous assay. The fluorescence intensity gradually increased with the raised concentration of Pb^{2+}.

Figure 4b shows the upconversion fluorescence intensity at 547 nm for the different concentrations of Pb^{2+}. The upconversion fluorescence intensity at 547 nm was

Table 1 Comparison between the developed biosensors for Pb^{2+} and other reported method

Method	Technique or material	Liner range (nM)	LOD (nM)	Ref
colorimetric	gold nanoparticle	1–1000	2.4	[35]
colorimetric	glutathione functionalized gold nanoparticles	100–10,000	100	[36]
Fluorescence	2-amino-5,6,7-trimethyl-1,8-naphthyridine	0–1000	4	[10]
Fluorescence	boron-doped carbon	25–250,000	8.47	[37]
Our method	UCNPs-MNPs-GNPs	25–1400	5.7	

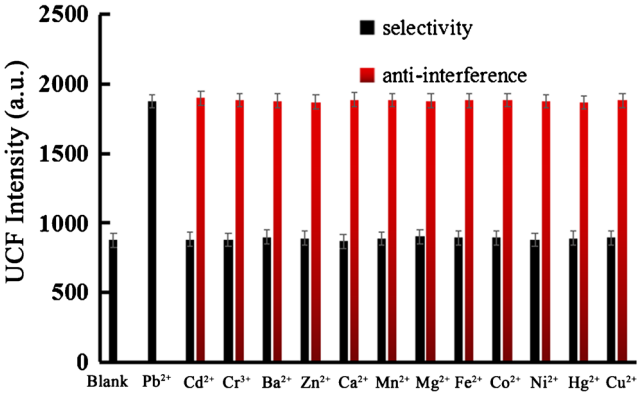

Fig. 5 The selectivity of the fluorescent nanoprobe for 1 μM Pb^{2+} against various kinds of 100 μM interference ions. Schematic presentation of fluorescent nanoprobe based on fluorescence resonance energy transfer (FRET) between upconversion (UCNPs) and gold nanoparticles (GNPs)-Fe_3O_4 magnetic nanoparticles (MNPs) for detection of Pb^{2+}

found to be linear with the concentration of Pb^{2+} ranging from 25 to 1400 nM, and the linear regression equation is $y = 1.212\ x + 677.29$ ($R^2 = 0.993$), The LOD (5.7 nM) can be calculated by $3S_b/S$ (S_b represents the standard deviation of 10 blank fluorescence measurements and S is the slope of calibration plot). A comparison between the developed nanoprobe and other reported methods [10, 35–37] for Pb^{2+} detection are summarized in Table 1. The above results confirmed that the developed method had high sensitivity in their detection.

The selectivity of the assay

As shown in Fig. 5, several metal ions (1 μM Pb^{2+} and 100 μM Cd^{2+}, Cr^{3+}, Ba^{2+}, Zn^{2+}, Ca^{2+}, Mn^{2+}, Mg^{2+}, Fe^{2+}, Co^{2+}, Ni^{2+}, Cu^{2+}, Hg^{2+}) were examined. The intensity at 547 nm had high only when Pb^{2+} was added, while other metal ions in 100 times were not able to initiate "turn-on" effect, demonstrated the high selectivity of our method. In addition, the results are also shown in Fig. 5. Almost the same upconversion fluorescence intensity was observed even with other metal ions, indicated other metal ions cannot influence the nanoprobe for Pb^{2+} detection.

Lead(II) determination in real samples

To evaluate the applicability of this nanoprobe in real samples, the UCNPs-MNPs-GNPs nanoprobe was used to measure Pb^{2+} in waste water and black tea and the results are shown in Table 2. Atomic absorption spectrometry (AAS) was used as a conventional method to verify the reliability of this nanoprobe. It was found that recoveries were in the range of 99.6 to 105.2% and the relative standard deviation (RSD) ($n = 3$) was less than 2.2. As illustrated in Table 2, the values determined by our suggested method were in good agreement with AAS. Therefore, it can be concluded that our approach would be suitable for practical application.

Conclusion

A new nanoprobe is described for Pb^{2+} detection in aqueous media, using DNAzyme as Pb^{2+}-capturing element, upconversion particles as fluorescence donors and MNPs-GNPs as fluorescence acceptor. The sensitivity of UCNPs-MNPs-GNPs nanoprobe can be impacted under the ratios of UCNPs and MNPs-GNP, hybridization time and reaction time after the addition of Pb^{2+} evidently. The newly prepared UCNPs-MNPs-GNPs nanoprobe had a specific fluorescence response to Pb^{2+} with a detection limit of 5.7 nM. Moreover, the obtained results for the detection of Pb^{2+} in water and black tea samples gave credence to its potential deployment for the safety monitoring of the toxic metals in food.

Table 2 Determination of Pb^{2+} in real sample using the developed method

Samples	Added amounts(nM)	Measured amounts [a] (nM)	Recovery (%)	RSD (%) n = 3	Measured amounts [b] (nM)
tap water	200	210.4 ± 0.31	105.2	2.2	211.2 ± 0.22
	400	408.6 ± 0.27	102.1	1.4	411.2 ± 0.31
	600	612.7 ± 0.41	102.1	0.9	615.7 ± 0.08
	800	796.4 ± 0.12	99.6	1.7	802.4 ± 0.51
Black tea	200	214.1 ± 0.37	107.0	1.3	217.3 ± 0.23
	400	412.3 ± 0.34	103.1	2.1	415.4 ± 0.17
	600	616.7 ± 0.22	102.8	0.8	608.3 ± 0.25
	800	812.4 ± 0.26	101.6	1.5	809.1 ± 0.39

[a] Values determined by the developed method

[b] Values determined by AAS

Acknowlegements This research is supported by the National Natural Science Foundation of China (31972154, 31901772), the 333 High-level Talents Project of Jiangsu Province (BRA2019087), the Key R&D Program of Jiangsu Province (BE2017357), and the China Postdoctoral Science Foundation (2019 M651748).

Compliance with ethical standards The author(s) declare that they have no competing interests.

References

1. Wen B, Xue J, Zhou X, Wu Q, Nie J, Xu J, Du B (2018) Highly selective and sensitive detection of Pb2+ in aqueous solution using tetra(4-pyridyl)porphyrin-functionalized Thermosensitive ionic microgels. ACS Appl Mater Interfaces 10:25706–25716
2. Niu X, Zhong Y, Chen R, Wang F, Liu Y, Luo D (2018) A "turn-on" fluorescence sensor for Pb2+ detection based on graphene quantum dots and gold nanoparticles. Sensors Actuators B Chem 255:1577–1581
3. Zhang D, Zhu M, Zhao L, Zhang J, Wang K, Qi D, Zhou Y, Bian Y, Jiang J (2017) Ratiometric fluorescent detection of Pb(2+) by FRET-based Phthalocyanine-Porphyrin dyads. Inorg Chem 56(23):14533–14539
4. Kim JH, Han SH, Chung BH (2011) Improving Pb2+ detection using DNAzyme-based fluorescence sensors by pairing fluorescence donors with gold nanoparticles. Biosens Bioelectron 26(5): 2125–2129
5. Khan NA, Niaz A, Zaman MI, Khan FA, Nisar-ul-haq M, Tariq M (2018) Sensitive and selective colorimetric detection of Pb2+ by silver nanoparticles synthesized from Aconitum violaceum plant leaf extract. Mater Res Bull 102:330–336
6. Choudhury R, Misra TK (2018) Gluconate stabilized silver nanoparticles as a colorimetric sensor for Pb 2+. Colloid Surface A 545: 179–183
7. Zhang B, Wei C (2018) Highly sensitive and selective detection of Pb 2+ using a turn-on fluorescent aptamer DNA silver nanoclusters sensor. Talanta 182:125–130
8. Zhang D, Zhu M, Zhao L, Zhang J, Wang K, Qi D, Zhou Y, Bian Y, Jiang J (2017) Ratiometric fluorescent detection of Pb2+ by FRET-based Phthalocyanine-Porphyrin dyads. Inorg Chem 56(23): 14533–14539
9. Ouyang H, Ling S, Liang A, Jiang Z (2018) A facile aptamer-regulating gold nanoplasmonic SERS detection strategy for trace lead ions. Sensors Actuators B Chem 258:739–744
10. Yu X, Aijun T, Yi L (2009) Abasic site-containing DNAzyme and aptamer for label-free fluorescent detection of Pb(2+) and adenosine with high sensitivity, selectivity, and tunable dynamic range. J Am Chem Soc 131(42):15352–15357
11. Shenshan Z, Yuangen W, Yanfang L, Le L, Lan H, Haibo X, Pei Z (2014) Label-free fluorescent sensor for lead ion detection based on lead(II)-stabilized G-quadruplex formation. Anal Biochem 462:19–25
12. Mou X, Wang J, Meng X, Liu J, Shi L, Sun L (2017) Multifunctional nanoprobe based on upconversion nanoparticles for luminescent sensing and magnetic resonance imaging. J Lumin 190:16–22
13. Wu B, Cao Z, Zhang Q, Wang G (2018) NIR-responsive DNA hybridization detection by high efficient FRET from 10-nm upconversion nanoparticles to SYBR green I. Sensors Actuators B Chem 255:2853–2860
14. Ouyang Q, Liu Y, Chen Q, Guo Z, Zhao J, Li H, Hu W (2017) Rapid and specific sensing of tetracycline in food using a novel upconversion aptasensor. Food Control 81:156–163
15. Li H, Ahmad W, Rong Y, Chen Q, Zuo M, Ouyang Q, Guo Z (2020) Designing an aptamer based magnetic and upconversion nanoparticles conjugated fluorescence sensor for screening Escherichia coli in food. Food Control 107:106761
16. Chen M, Kutsanedzie FYH, Cheng W, Agyekum AA, Li H, Chen Q (2018) A nanosystem composed of upconversion nanoparticles and N, N-diethyl-p-phenylenediamine for fluorimetric determination of ferric ion. Microchim Acta 185(8):378
17. Chen M, Kutsanedzie FYH, Cheng W, Li H, Chen Q (2019) Ratiometric fluorescence detection of Cd2+ and Pb2+ by inner filter-based upconversion nanoparticle-dithizone nanosystem. Microchem J 144:296–302
18. Li X, Wu Y, Liu Y, Zou X, Yao L, Li F, Feng W (2014) Cyclometallated ruthenium complex-modified upconversion nanophosphors for selective detection of Hg2+ ions in water. Nanoscale 6(2):1020–1028
19. Ding N, Cao Q, Zhao H, Yang Y, Zeng L, He Y, Xiang K, Wang G (2010) Colorimetric assay for determination of lead (II) based on its incorporation into gold nanoparticles during their synthesis. Sensors-Basel 10(12):11144–11155
20. Zhang H, Zhang Y, Jin R, Wu C, Zhang B, Zhang Q, Chen X (2018) Preparation and photothermal therapy of hyaluronic acid–conjugated au nanoparticle-coated poly (glycidyl methacrylate) nanocomposites. J Mater Sci 53:16252–16262
21. Dai D, Xu D, Cheng X, He Y (2014) Direct imaging of single gold nanoparticle etching: sensitive detection of lead ions. Anal Methods 6(13):4507–4511
22. Mou Y, Yang H, Xu ZL (2017) Morphology, surface layer evolution and structure-dye adsorption relationship of porous Fe3O4 MNPs prepared by solvothermal/gas generation process. ACS Sustain Chem Eng 5(3):2339–2349
23. Demin AM, Mekhaev AV, Esin AA, Kuznetsov DK, Zelenovskiy PS, Shur VY, Krasnov VP (2018) Immobilization of PMIDA on Fe 3 O 4 magnetic nanoparticles surface: mechanism of bonding. Appl Surf Sci 440:1196–1203
24. Singh P, Upadhyay C (2018) Role of silver Nanoshells on structural and magnetic behavior of Fe 3 O 4 nanoparticles. J Magn Magn Mater 458:39–47
25. Zhao Y, Xie X, Zhao Y, Xie X (2017) A novel electrochemical Aptamer biosensor based on DNAzyme decorated au@Ag Core-Shell nanoparticles for Hg2+ determination. J Braz Chem Soc 29(2):232–239
26. Wang Q, Yang XH, Wang L, Wang KM, Zhao X (2007) Novel fluorescent probe for lead ion detection based on DNAzyme. Chem J Chin Univ 28(12):2270–2273
27. Chen Q, Hu W, Sun C, Li H, Ouyang Q (2016) Synthesis of improved upconversion nanoparticles as ultrasensitive fluorescence probe for mycotoxins. Anal Chim Acta 938:137–145
28. Hu W, Chen Q, Li H, Ouyang Q, Zhao J (2016) Fabricating a novel label-free aptasensor for acetamiprid by fluorescence resonance energy transfer between NH2-NaYF4: Yb, Ho@SiO2 and Au nanoparticles. Biosens Bioelectron 80:398–404
29. Li H, Chen Q, Hassan MM, Ouyang Q, Jiao T, Xu Y, Chen M (2018) AuNS@Ag core-shell nanocubes grafted with rhodamine for concurrent metal-enhanced fluorescence and surfaced enhanced Raman determination of mercury ions. Anal Chim Acta 1018:94–103
30. Shijia W, Nuo D, Zhouping W, Hongxin W (2011) Aptamer-functionalized magnetic nanoparticle-based bioassay for the detection of ochratoxin a using upconversion nanoparticles as labels. Analyst 136(11):2306–2314
31. Liu Y, Ouyang Q, Li H, Chen M, Zhang Z, Chen Q (2018) Turn-on Fluoresence sensor for Hg2+ in food based on FRET between Aptamers-functionalized Upconversion nanoparticles and gold nanoparticles. J Agric Food Chem 60:6188–6195

32. Erdemoğlu SB, Pyrzyniska K, Güçer Ş (2000) Speciation of aluminum in tea infusion by ion-exchange resins and flame AAS detection. Anal Chim Acta 411(1):81–89
33. Liu Y, Ouyang Q, Li H, Zhang Z, Chen Q (2017) Development of an inner filter effects-based Upconversion nanoparticles-Curcumin Nanosystem for the sensitive sensing of fluoride ion. ACS Appl Mater Interfaces 9(21):18314–18321
34. Sun C, Li H, Koidis A, Chen Q (2016) Quantifying Aflatoxin B1 in peanut oil using fabricating fluorescence probes based on upconversion nanoparticles. Spectrochimica acta. Spectrochim Acta B 165:120–126
35. Shahdordizadeh M, Yazdian-Robati R, Ansari N, Ramezani M, Abnous K, Taghdisi SM (2018) An aptamer-based colorimetric lead(II) assay based on the use of gold nanoparticles modified with dsDNA and exonuclease I. Microchim Acta 185(2):151
36. Chai F, Wang C, Wang T, Li L, Su Z (2010) Colorimetric detection of Pb2+ using glutathione functionalized gold nanoparticles. ACS Appl Mater Interfaces 2(5):1466–1470
37. Wang ZX, Yu XH, Li F, Kong FY, Lv WX, Fan DH, Wang W (2017) Preparation of boron-doped carbon dots for fluorometric determination of Pb(II), cu(II) and pyrophosphate ions. Microchim Acta 184(12):4775–4783